RSC Advances

ROYAL SOCIETY OF CHEMISTRY

www.rsc.org/advances

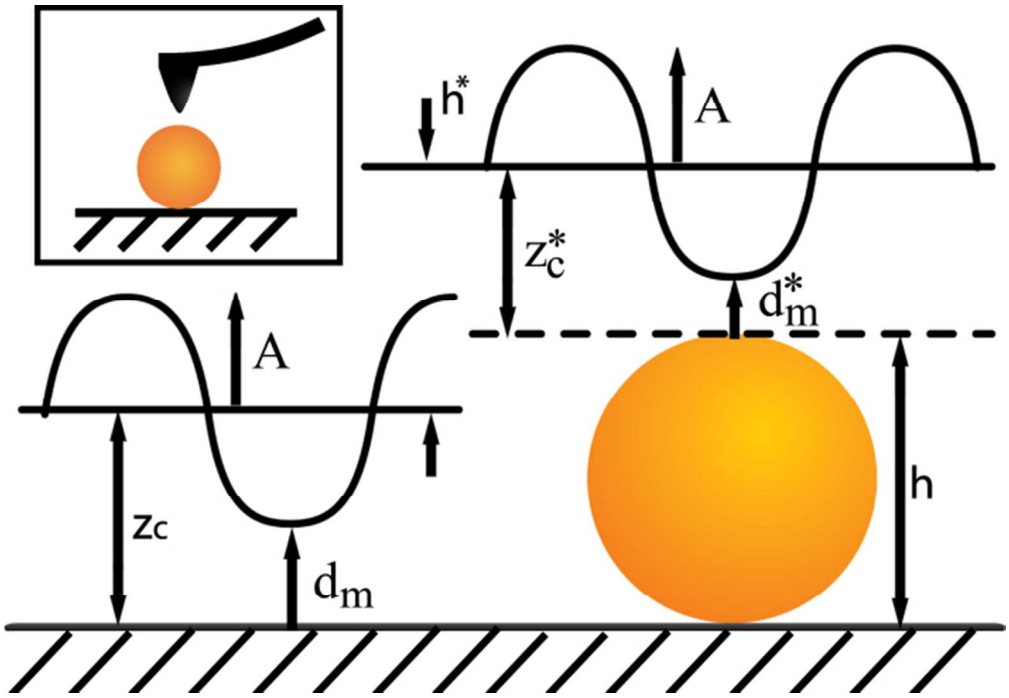

120x82mm (150 x 150 DPI)

General interpretation and theory of apparent height in dynamic atomic force microscopy

Chia-Yun Lai, Sergio Santos, Matteo Chiesa

Laboratory for Energy and NanoScience (LENS), Institute Center for Future Energy (iFES), Masdar Institute of Science and Technology, Abu Dhabi, UAE

Abstract

We provide a general theory and interpretation behind the ubiquitous loss of apparent height of nanostructures in dynamic atomic force microscopy that occurs in the attractive regime irrespectively of stiffness. We show analytically and numerically that while the true height of a nanostructure could be smaller than measured, lack of symmetry biases measurements towards height loss. In particular, the finite size of the tip always contributes to height loss while the nature of attractive forces might contribute to height gain or loss. The theory further predicts otherwise counterintuitive phenomena such as the possibility to gain height by increasing the interaction.

Keywords: height, nanoscale, dimension, afm

I. INTRODUCTION

The fields of nanosciences and nanotechnology are based upon the finite size of nanostructures and the properties that follow from their dimensions[1]. Therefore characterizing the dimensions of nanostructures with precision and accuracy is instrumental in order to fine-tune, predict and employ their properties and function[2-4]. In principle, the atomic force microscope AFM is very well suited and currently the only instrument with sub-nm[5] or even sub-angstrom precision to measure the height of nanostructures[6]. Nanostructures such as nanoparticles[7], isolated DNA[8, 9] and/or proteins[10], carbon nanotubes CNTs[11], etc. are typically dispersed on hard surfaces and the apparent width and height are recorded via topographic AFM maps. Arguably however, it is still to be conclusively shown that obtaining the true height of a nanostructure with sub-angstrom margin of error is possible, whether directly[12] or indirectly[5, 13-15], from the experimental observables in the measurement[16]. Probing soft matter is even more challenging because of the added difficulty of imaging feeble systems[12, 13, 15]. Furthermore, while dynamic AFM (dAFM) modes of operation, such as amplitude and frequency modulation (AM and FM AFM), have arguably minimized the problems related to sample deformation and damage, these are still considerable and depend on the mode of operation and parameters being used[8, 9, 15, 17, 18].

In short, the interpretation of apparent height of isolated nanostructures[19] is currently based on a varied range of mechanisms such as peak forces and deformation[15, 20], adsorbed contamination and water on the supporting surface[21, 22], the nature and origin of the nanoscale forces[18, 19], tip-sample stochastic or permanent damage[23] and even artifacts related to cantilever dynamics[24]. Despite these complications, apparent height measurements are a fundamental aspect of the technique and are commonly employed as a benchmark to validate

the performance of imaging modes[12, 14] and draw physical and biologically relevant conclusions[25-27]. Analytical formulae that yield both qualitative and quantitative information however, are still missing[8, 16, 19] or, at best, based on mechanical deformation [7, 11, 15, 28]. Here, we develop a force independent theory of apparent height in dAFM that can be written in terms of the general expressions of dAFM[29-31] and the respective experimental observables[30, 31]. Then, we set to derive close form formulae to directly quantify height loss in the absence of sample deformation which is the preferred method to non-invasively image soft isolated nanostructures supported onto flat surfaces.

II. RESULTS AND DISCUSSION

A. General theory of height reconstruction in dynamic AFM

Fig 1 is employed to illustrate the process of height reconstruction in dAFM. In the figure we show the ideal case of an isolated spherical sample of height h, or radius R_s ($h=2R_s$), supported onto a flat surface. We have chosen a spherical sample for simplicity and also because it helps to intuitively understand the importance of geometry in the process of apparent height formation. Furthermore, the way to generalize to other geometries should be apparent from this derivation, even if the expressions might become cumbersome[32]. We assume that the tip oscillates in the non-contact mode (nc-mode), or regime, throughout, that is, in the absence of mechanical contact with the sample. We further distinguish between the tip-supporting surface interaction and the tip-sample interaction. Sample refers to the isolated nanostructure throughout. Then, absent sample there is only tip-supporting surface (or tip-surface) interaction (left in Fig. 1). Present sample there is tip-sample and tip-surface

interaction (right in Fig. 1) where the tip-surface interaction can be regarded as a background signal[16, 19]. Assuming first the case of absent sample where the tip is raster scanning the surface from left to right, a given cantilever-surface separation z_c follows for a prescribed amplitude A. Typically $z_c/A>1$ for nc-mode imaging. Then, present sample, the cantilever oscillates with separation z^*_c+h relative to the supporting surface and z^*_c relative to the sample's top surface. The apparent height is given by

$$h^* = h + \Delta h \equiv h + \Delta z_c \quad (1)$$

where $\Delta h=h^*-h$ is the error in height and it is numerically equal to $\Delta z_c=z^*_c-z_c$ (Fig. 1). If $\Delta z_c=0$, the measured apparent height and the true height coincide. The physical phenomena leading to nonzero values in Δh are discussed next.

The oscillation amplitude in AM AFM is controlled by the virial V[30] and the energy irreversibly dissipated in the tip-sample junction E_{ts}[33, 34] in the interaction. Both terms can be written in terms of observables (see supplementary information). In the presence of conservative interactions only, $E_{ts}=0$ and then V alone is responsible for the amplitude decay or topography measurements[30]. Here we assume that $E_{ts}=0$ throughout and focus on the contribution from V only while recalling that irreversible losses of energy ($E_{ts}>0$) are indicative of invasiveness. Furthermore, we caution the reader that a theory including energy dissipation would be required in cases where E_{ts} cannot be ignored. By employing V alone however, there is the added advantage that the theory is applicable to both standard AM AFM and FM AFM. We note that it has long been known that the virial V alone controls the relationship between cantilever separation z_c and frequency shift, i.e. topography in FM AFM[31, 35], and z_c and A (absent dissipation), i.e. topography in AM AFM[36]. Furthermore ignoring the contribution from E_{ts} greatly simplifies the analysis when considering close form

expressions (see supplementary for details). The virial expression V is well known, established in the literature as a general expression in dAFM[30, 31] and corresponds to the time averaged product between the force F_{ts} and the deflection z (z_0 is the mean deflection), where $z(t) \approx z_0 + A\sin(\omega t+\phi)$, producing

$$V(z_c) \equiv V_{sur}(z_c) = -\frac{kA(z_c)A_0}{2Q}\cos\phi(z_c) \approx \frac{kA_r A_0^2}{2Q}\sqrt{1-A_r^2} \quad (2)$$

where k is the spring constant, Q is the quality factor, ϕ is the phase shift and the suffix sur implies tip-supporting surface interaction in the absence of the sample (Fig. 1). The cosine of ϕ can be written in terms of the amplitude ratio $A_r=A/A_0$ because zero dissipation is assumed[37]. Present sample there are two contributions to the virial V (Fig. 1); 1) the tip-supporting surface interaction $V_{sur}(z^*_c+h)$ and 2) the tip-sample interaction $V_{sam}(z^*_c)$ where the suffix sam stands for the tip-sample pair. In the presence of the sample, the net virial $V_{sur-sam}$ can be written as the contribution between the two

$$V_{sur-sam}(z_c^*, h) \equiv V_{sur}(z_c^* + h) + V_{sam}(z_c^*) \quad (3)$$

Then, a constraint to the apparent height h^* follows from (2) and (3) producing

$$V_{sur-sam}(z_c^*, h) = V_{sur}(z_c) = \frac{kA_r A_0^2}{2Q}\sqrt{1-A_r^2} \quad (4)$$

At this point it is worth noting that Eq. (4) is general for any tip-sample interaction in AM AFM in the absence of dissipative phenomena and general in FM AFM where conservative interactions control the feedback independently of whether there is irreversible loss of energy. Furthermore, from (4), it follows that the pair z^*_c and z_c give place to a given error $\Delta z=\Delta h$ (Fig. 1) that depend on A, A_0, k and Q, i.e. operational and cantilever parameters respectively. Thus, practically, the measured apparent height depends on the choice of

operational parameters and the cantilever chosen to perform the experiment. From this it follows that different values of apparent height might follow in different experiments thus explaining the variability of measured values of apparent height with operational parameters and cantilever models reported in the literature[20, 38, 39].

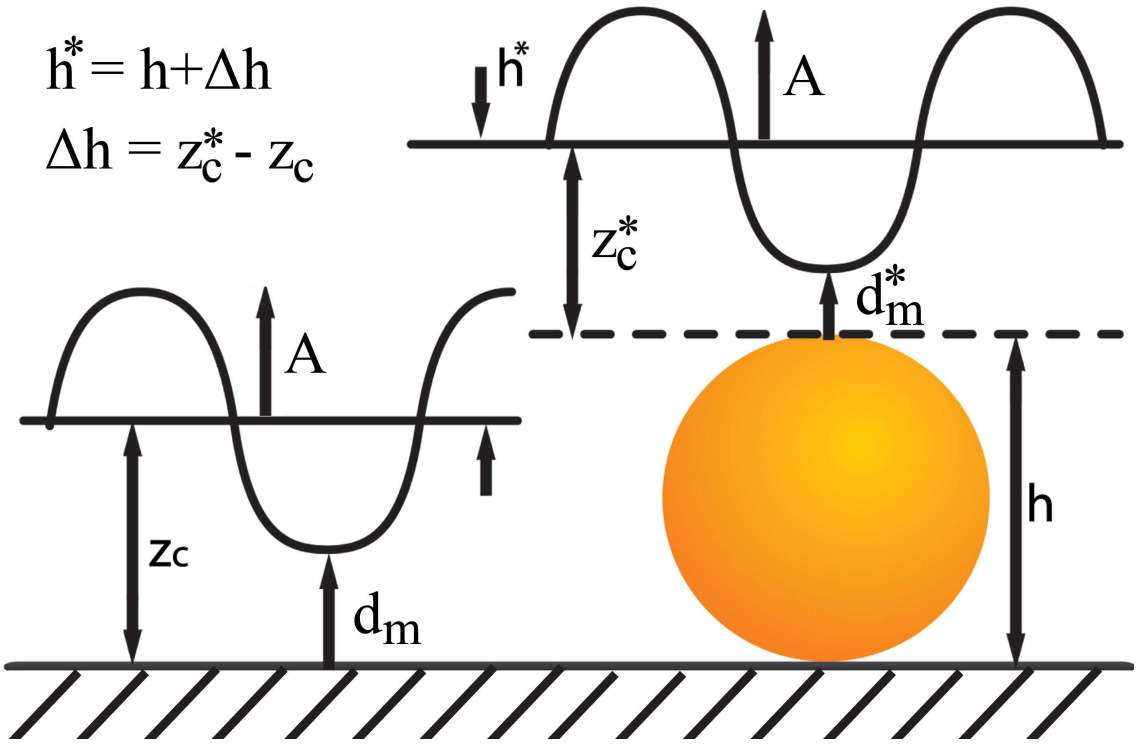

FIG. 1 Scheme of apparent height reconstruction where h is the true height of a sphere of radius R_s and h^* is the apparent height as obtained in dynamic AFM. The scheme shows the minimum distances of approach d_m and d_m^* in the absence and presence of the spheric sample respectively.

B. Model based analytic expression for height recovery in nc AFM

In order to derive a close form analytical expression for the error in height that takes into account geometry and sample properties a model for the force is next employed. We select a model that constrains the forces to be directly proportional to the tip radius R, inversely proportional to the square of the distance d and where both tip and sample can be modelled as spheres. Such force model is in agreement with the ubiquitous London dispersion, Debye and Keesom forces for the van der Waals interactions[32], and can be written following Hamaker's approach[32, 40]. Furthermore, from now on, we will refer to the chemistry of the system by employing the concept of Hamaker constant H (which depends on the atomic composition of the tip, sample and supporting substrate) as originally done by Hamaker. H is a constant of proportionality in the force. Taking into account the above constraint, absent sample, the force is

$$F_{sur} = -\frac{R_t H_{sur}}{6d^2} \qquad a_0<d \qquad (5)$$

where R_t is the tip radius, a_0 is an intermolecular distance, H_{sur} is H for the tip-supporting surface interaction, d is the instantaneous tip sample distance and $d=z_c+z$. For this force, and by computing its virial[36], the resulting cantilever separation z_c can be written as

$$z_c \approx A\left(D_{sur}\left[1-\frac{z_c z_0}{A^2}\right]^{2/3}+1\right)^{1/2} \qquad (6)$$

where D contains the cantilever-surface properties since

$$D=\sqrt[3]{\frac{\left(\frac{QR_t H_{sur}}{3kA_0^3}\right)^2}{\left(A_r^4-A_r^6\right)}} \qquad (7)$$

An approximation of (6) can be derived by ignoring z_0, i.e. $z_c z_0/A^2 \ll 1$. This condition applies in many cases of interest and allows finding the cantilever separation explicitly[29, 30]

$$z_c \approx A(D+1)^{1/2} \tag{8}$$

The presence of a sample (Fig. 1 and discussion) gives rise to a contribution from the tip-supporting surface and tip-sample pairs[16]

$$F_{sam} = -\frac{R_t H_{sur}}{6d^2} - \frac{R^* H_{sam}}{6(d-h)^2} \tag{9}$$

where

$$R^* \approx \frac{R_t R_s}{R_t + R_s} \tag{10}$$

Where H_{sam} corresponds to the tip-sample system H. The net (virial neglecting the z_0) of (9) can be written as (see supplementary)

$$\left[\left(\frac{z_c^* + h}{A}\right)^2 - 1\right]^{-3/2} + H_r R_r \left[\left(\frac{z_c^*}{A}\right)^2 - 1\right]^{-3/2} \approx D^{-3/2} \tag{11}$$

where

$$H_r = \frac{H_{sam}}{H_{sur}} \;;\; R_r \equiv \frac{R^*}{R_t} = \frac{R_s}{(R_s + R_t)} \tag{12}$$

By combining (8) and (11) the error in height Δh can be found implicitly. We can find a simpler and explicit solution for the error in height Δh however by ignoring the background interaction with the surface $V_{sur}(z^*_c, h)$ in (11) giving

$$z_c^* \approx A\left(\left(H_r R_r\right)^{2/3} D+1\right)^{1/2} \tag{13}$$

Then Δh follows from combining (8) and (13)

$$\Delta h \equiv z_c^* - z_c \approx A\left[\left(\left(H_r R_r\right)^{2/3} D+1\right)^{1/2} - \left(D+1\right)^{1/2}\right] \tag{14}$$

The expression in (14) is sufficiently simple that qualitative information about the error in height Δh can be deduced directly by inspection. From (14), we distinguish between several important possibilities. First, the error in apparent height Δh will be zero if and only if H_rR_r=1. Importantly this is true irrespectively of operational and cantilever parameters since these depend on D only. Furthermore since R_r<1 always, i.e. $R_r \rightarrow 1$ when $R_t \rightarrow 0$ because of the finite size of the tip, it follows that the contribution from R_r (geometry) in H_rR_r will always lead to height loss. Second, the condition H_r=1 requires that the tip-surface chemistry H_{sur} is the same as the tip-sample chemistry H_{sam}. Third, the condition H_rR_r >1 is physically meaningful and implies that a suitable choice of chemistry can lead to gain in apparent height, i.e. Δh>0. Furthermore, a counterintuitive effect might occur when H_rR_r>1, i.e. the tip required to recover the true height might not necessarily be the sharpest. That is, from (14), the condition for zero error Δh=0 when H_r >1 is

$$H_r = \frac{1}{R_s} \tag{15}$$

or

$$R_t = R_s\left(H_r - 1\right) \tag{16}$$

Fourth, provided $H_r \leq 1$, the tip should be sharpest in order to measure a height as close as possible to the true height. Finally, we recall that Eq. (14) is valid provided the interaction with the supporting surface in the presence of the sample is small enough, i.e. $V(z^*_c)$/ V_{sur}-

$_{sam}(z^*_c, h)<<1$. If $V(z^*_c)$ cannot be ignored, then the fundamental expressions in (8) and (13) should be considered. The mean deflection should further be considered when the condition $z_c z_0/A^2<<1$ does not apply, i.e. for example under liquid environments[41]. An implicit expression can also be written for these cases (see supplementary Eq. (S9)).

C. Numerical analysis and validation of the theory

In order to establish the validity of the above analytical theory the standard equation of motion for modeling the dynamics of the cantilever in dAFM, i.e. a mass on a spring with a non-linear force and with linear damping with the medium[42], has been solved numerically (fourth order Runge Kutta algorithm, see supplementary for details). In Fig. 2, a ratio $H_r=1$ (same chemistry throughout) has been set implying that any loss of height is due solely to the contribution from R_r. The sample's radius has been set to $R_s=1$ nm since this is the size of benchmark systems such as DNA molecules[38, 39] and close to the height of small proteins[10, 15, 17] and other nanostructures[11]. The tip radius is $R_t=20$ (dashed dotted), 2 (dashed) and 0.2 (continuous) nm resulting in $R_r=0.83$, 0.33, 0.05. The remaining parameters are: $A_0=$ 1nm, k=40 N/m, $f_0=300$ kHz and Q=500, resulting in $d>a_0$ throughout (nc regime).

The results in Fig. 2a show that the approximation in (8) for z_c together with the approximation in (11) for z_c^* (markers) lead to minor errors in h^*, i.e. less than 1%, relative to the numerical results (lines). The second approximation corresponds to that in (8) for z_c together with that in (13) for z_c^* (markers), where the contribution from the surface was ignored in the presence of the sample (Fig. 2b). Several outcomes are worth mentioning. First, for all values of R_r, the approximation in (13) and (14) improves with decreasing

amplitude ratio A_r. This can be attributed to a decreasing contribution from the surface to the net virial as shown in Fig. 2c -note that in Fig. 2c the corresponding normalized virial $V_{sur}/V_{sur\text{-}sam}$ is plotted as a function of A_r. Large values of normalized virial correspond to large contribution from the tip-surface interaction in the presence of the sample while low values correspond to small contributions. Second the approximation improves as R_r tends to 1, i.e. as the tip becomes sharper (Fig. 2b). That is, users concerned with the use of the approximation in (13) should carefully select the sharpest tips possible, i.e. 2- 5 nm or less. In Fig. 2, all the height loss is influenced by the ratio $R_r<1$, i.e. the finite size of the tip, since $H_r=1$. It is also remarkable that an increasing interaction, i.e. decreasing amplitude ratio A_r, typically leads to larger values of apparent height. This is a counterintuitive result that implies that gentle interactions do not necessarily lead to larger values of apparent height as typically interpreted in the literature[12, 14, 15].

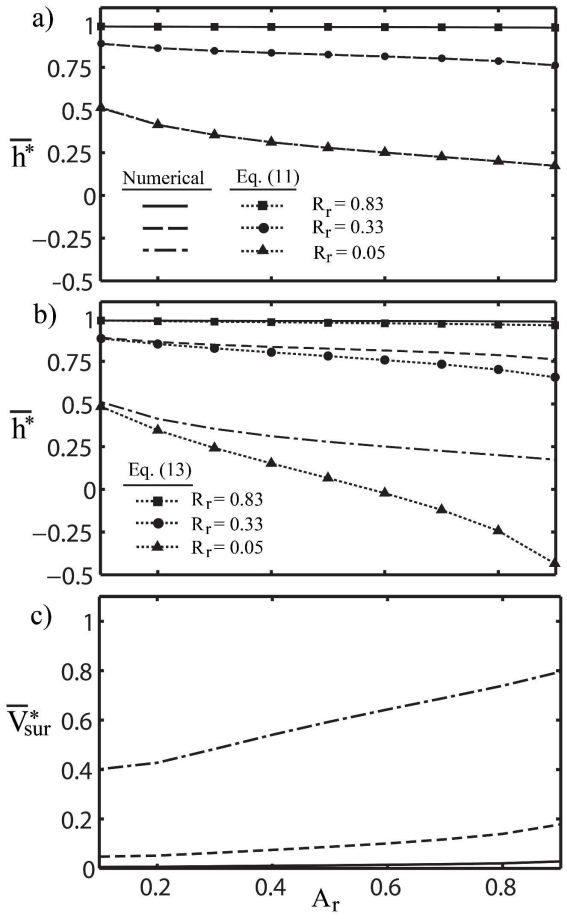

FIG. 2 Simulations and analytical expressions showing the effects of varying the tip radius R_t in the nc mode as a function of $A_r=A/A_0$ on the normalized apparent height h^*/h. a) and b) normalized apparent height h^*/h according to numerical results (lines) and approximations (markers). The approximations correspond to Eqs. (8) and (11) and (8) and (13) respectively. c) Normalized contribution to the Virial from the surface in the presence of the sample $V_{sur}/V_{sur\text{-}sam}$.

Next the influence of H_r is explored with the help of Fig.3. Here R_r has been set to 0.17 throughout and the other parameters, except for H_r, are the same as those in Fig. 2. Physically, this interaction corresponds to a sharp tip R_t=5 nm imaging a small spheres R_s= 1nm with varying Hamaker ratio H_r, i.e. heterogeneous chemistry. In the figure, H_r takes the values 10 (dashed dotted lines), 1 (dashed lines) and 0.1 (continuous lines). Again, the

approximations from (8) and (11) are shown with markers in Fig. 3a and the approximations from (8) and (13) are shown with markers in Fig. 3b. The corresponding virial relationship obtained from the numerical results is also shown in Fig. 3c. The interpretation of varying H_r is equivalent to that of varying R_r in Fig. 2 except for a remarkable difference. This difference relates to the variations in h^* with decreasing amplitude ratio R_r. In particular, the apparent height h^* increases with decreasing A_r if and only if $H_r>1$ (squares in Figs. 3a and 3b). Experimentally, this provides a simple method to deduce whether $H_r< \sim 0.1\text{-}1$ (higher chemical affinity between the tip and the supporting surface than between the tip and the sample) or $H_r> \sim 10$ (lower chemical affinity between the tip and the supporting surface than between the tip and the sample) provided the tip is sharp enough.

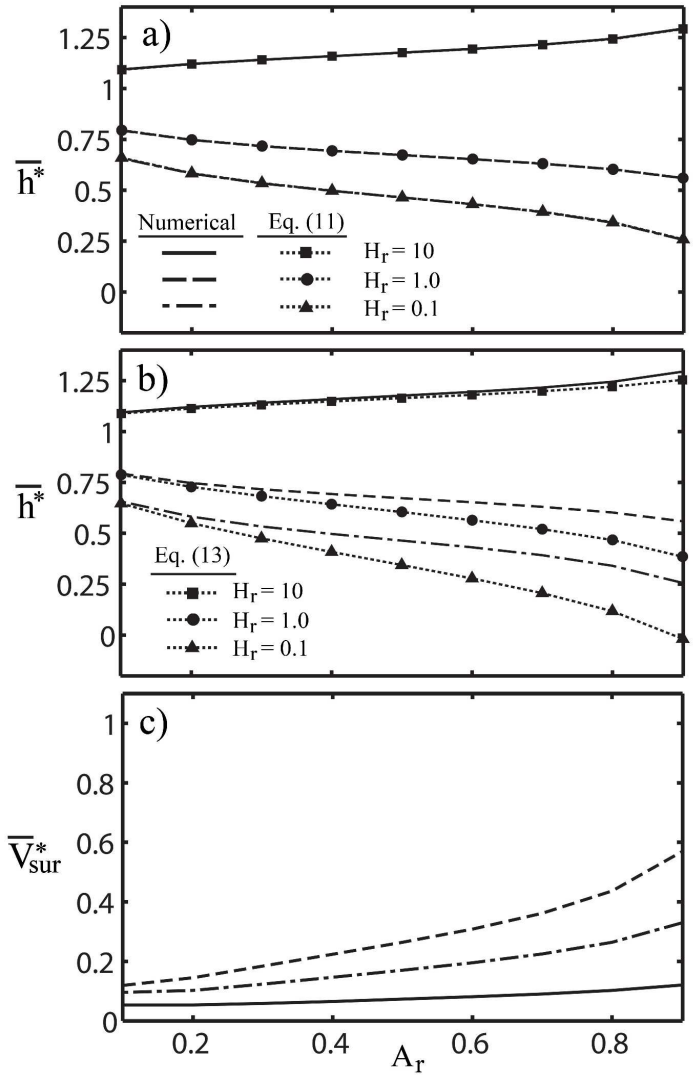

FIG. 3 Simulations and analytical expressions showing the effects of varying the ratio H_r in the nc mode as a function of $A_r=A/A_0$ on the normalized apparent height h^*/h. a) and b) normalized apparent height h^*/h according to numerical results (lines) and approximations (markers) as in Fig. 2. c) Normalized contribution to the Virial due to the interaction with the surface in the presence of the sample $V_{sur}/V_{sur\text{-}sam}$.

At this point, it is worth noting some remarks regarding the results of Figs. 2 and 3 and the assumptions so far. First, besides the assumptions already stated above, the results in Figs. 2 and 3 predict the apparent height as a function of A_r in the true non-contact regime, i.e. when mechanical contact with neither the sample nor the surface occurs. For example, the attractive regime is typically defined as the force regime for which the average force per cycle is negative[43] while here, non-contact implies not only that the average force is negative but that mechanical contact is never established in one cycle. The true nc regime is typically reached in AM AFM by sufficiently decreasing the free amplitude A_0[43, 44]. Second, it is constructive to analyze the relevance of the radius of the sample R_s relative to height loss. In particular, when R_s is much larger than the decay length λ of the interaction, i.e $R_s >> \lambda$, the contributions to losses in apparent height from the phenomena discussed here becomes negligible. This has already been recently shown by some via numerical methods[16, 19, 45]. Furthermore, the decay length λ of van der Waals forces affecting either the amplitude decay or the frequency shift in standard dynamic AFM is of either sub-nm[46] or a few nm at most, even in liquids[47] or in the presence of water layers on surfaces when imaging in ambient conditions[48]. Thus, when the radius of the sample lies in the order of several nm or more, the effects discussed in this work, i.e. loss in apparent height due to either chemistry or the finite size of the tip and the sample, should become negligible. In summary, larger values of R_s have not been taken into account because of the diminishing influence of the phenomena discussed here with increasing R_s.

D. Model systems: nanoparticles and DNA

Next we discuss some scenarios that correspond to typical interactions and experimental set-ups in AFM. We start with nanoparticles as isolated model samples dispersed on flat and hard surfaces[7, 49, 50]. Two interactions are explored for this case; an aluminum nanoparticle supported on 1) a silica surface (continuous lines) and 2) a Silicon Nitride (SiN_3) surface (dashed lines) (Fig. 4). The parameters of the simulations are: H_r are H_r=1.53 and 0.96 for the silica and the Silicon Nitride surfaces respectively[32], R_t= 5 nm, R_s=1 nm and rest of parameters are as in Figs. 2 and 3. The predictions of the analytical expressions (8) and (11) are shown in Fig. 4a with the use of squares and circles respectively for the two cases. The numerical predictions match the predictions of (8) and (11) to less than 1% in error. The predictions of the more restrictive analytical expressions (8) and (13) are shown in Fig. 4b. It is again observed that the errors now range from 5 to 15% relative to the numerical results, depending on A_r. In general, for standard values of set-point in AM AFM, i.e. A_r=0.2-0.9, it is expected that measured apparent heights will be ~10-20 % lower than the true heights for silica surfaces and ~15-30 % lower than the true heights for the Silicon Nitride surfaces. That is, in general nanoparticles imaged under these conditions will produce values of apparent height lower than the true height even in the absence of mechanical deformation.

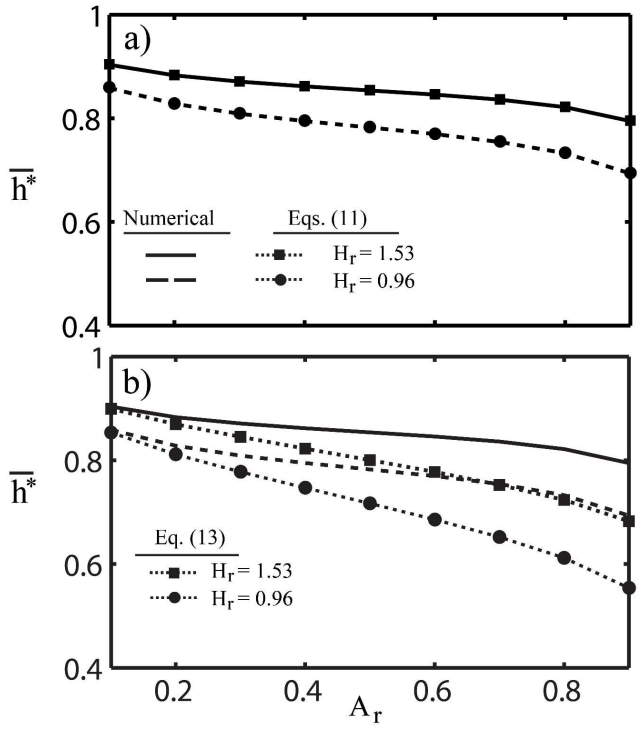

FIG. 4 Simulations and analytical expressions showing the effects of varying $A_r=A/A_0$ on the normalized apparent height h^*/h of a silicon tip interacting with an aluminum nanoparticle supported on 1) a silica surface and 2) a Silicon Nitride (SiN_3) surface (dashed lines and dashed lines with circles). In a) the numerical results (lines) are compared to the approximation of (8) and (11) (dashed lines and squares). In b) the numerical results (lines) are compared to the approximation of (8) and (13) (dashed-lines and circles).

A second case is shown in Fig. 5 where the model system is now a sphere of radius R_s=1 nm and a tip of radius R_t= 5, 10 and 20 nm. The values of the Hamaker constants are are H_{sam}= 35 zepto Joules and H_{sur} = 135 zepto Joules producing R_r=0.17 and H_r=0.26. These values for the H constants correspond to a silicon tip –mica surface interaction H_{sur} and a silicon tip-DNA interaction in ambient conditions according to recent studies performed both in AM AFM [44] and FM AFM [8, 45]. We further note that mica is a typical supporting surface for imaging isolated DNA in dynamic AFM. Modeling a DNA molecule as a single sphere of

R_s= 1 nm produces a lower bound in apparent height while modeling it as a cylinder of diameter 2 nm or a chain of contiguous 2 nm diameter spheres produces an upper bound. That is, the values obtained with better models that take the actual geometry of a DNA molecule into account should lie in between the values produced via these two simpler models. Moreover, since the values obtained with these two different models agree relatively well according to Cerreta et al.[8, 45], the simple model of a single sphere is employed here for simplicity for the ideal case of a spherical AFM tip imaging a DNA molecule. Selecting R_t=5 nm, i.e. a relatively sharp tip, further offers the advantage of reducing errors from the approximation in (13) as shown in Fig. 2b. But the three values of R_t are employed here as representative examples of standard tip radii employed experimentally. The results of numerically integrating the equation of motion are shown with the used of continuous lines, dashed lines, and dash-dotted lines for the three respective values of R_r (Fig. 5). The rest of parameters in the simulations are the same as in Fig. 4. The predictions of the analytical expressions (8) and (11) are shown in Fig. 5a with the use of squares, circles and triangles respectively for the three values of R_r. Again, the numerical predictions match the predictions of (8) and (11) to less than 1% in error. The predictions of the more restrictive analytical expressions (8) and (13) are shown in Fig. 5b and are once more larger, in agreement with the results above. The main practical conclusions that can be drawn from the results in Fig. 5 are; 1) for standard values of set-point in AM AFM, i.e. A_r=0.2-0.9, it is expected that measured apparent heights of DNA will be ~20-40 %, ~30-60 % and ~50-80 % lower than the true height of DNA, i.e. ~ 2nm, for R_t= 5 (squares), 10 (circles) and 20 (triangles) nm respectively. In summary, the predictions are in agreement with the varied range of DNA heights typically reported in the literature[5, 21, 38, 45]. These results further imply that the user should monitor the tip radius and take it into account, possibly maintaining it as sharp as

possible in order to obtain close to true values, when drawing conclusions[25, 51] about apparent height and true height.

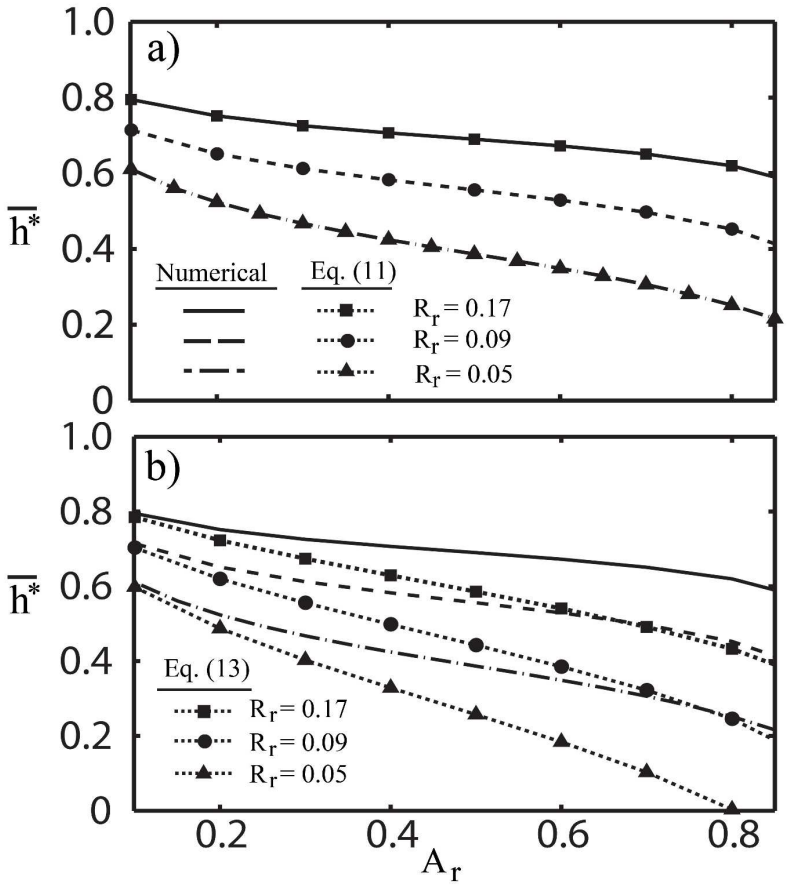

FIG. 5 Simulations and analytical expressions showing the effects of varying $A_r=A/A_0$ on the normalized apparent height h^*/h of a silicon tip interacting with an aluminum nanoparticle supported on 1) a silica surface and 2) a Silicon Nitride (SiN_3) surface (dashed lines and dashed lines with circles). In a) the numerical results (lines) are compared to the approximation of (8) and (11) (dashed lines and squares). In b) the numerical results (lines) are compared to the approximation of (8) and (13) (dashed-lines and circles).

As a final note to the use of the very small free amplitudes, i.e. A_0~ 1nm, employed in this work we recall that very small free amplitudes are typically necessary to stay in the true non-contact mode of operation, i.e. where van der Waals forces dominate[52]. In practice, the sharper the tip the smaller the value of A_0 required to stay in the true non-contact mode, and as a rule of thumb, the value of A_0 to stay in the true-non-contact mode should be smaller than a quarter of the free amplitude required to reach the repulsive regime[52]. The stiffness of the cantilever should also be considered in the sense that the smaller the value of A0 employed the larger the value of spring constant k necessary to obtain stable tip oscillations[53]. We would also like to emphasize that the fact that we have employed the ubiquitous inverse square law for the van der Waals forces in section II.B, i.e. predicted by London, Debye and Keeson interactions, for simplicity and generality. Any other models, such as those accounting for electrostatic interactions should develop section II. B in full for the selected force. On the other hand, the theory in section II. A is general for dynamic AFM and should form the base of the theories.

III. CONCLUSIONS

In summary, we have derived general analytical expressions that can be employed to understand the physical origin of the reconstructed topography in dynamic atomic force microscopy for soft isolated nanostructures on flat surfaces. With the use of suitable models and reasonable approximations it is also possible to recover the true height, or equivalently finding the error in height, and the contributions from geometrical and chemical factors. We acknowledge however that these results are more restrictive since the actual force profile should be known. In short, our results indicate that the range in apparent height values reported in the literature for isolated nanostructures, i.e. DNA, nanoparticles, proteins, etc.,

are consistent with the complex interplay between geometry and chemistry that controls the resulting apparent height in a given measurement. Furthermore, in the absence of mechanical deformation the apparent height might increase with increasing interaction, i.e. by lowering the amplitude ratio, a result that is counterintuitive and largely ignored in the literature. Finally, these results might lead to fine tuning apparent height measurements and suitable functionalizing supporting surfaces in order to obtain close to true values of apparent height.

References

1. R. M. Brydson, C. Hammond, D. Mowbray, M. R. J. Gibbs, I. Todd, M. Grell, I. W. Hamley, M. Geoghegan, R. A. L. Jones and G. J. Leggett, *Nanoscale Science and Technology*, Wiley, Chichester, 2005.
2. *Nature*, 2011, **476**, 374-374.
3. A. K. Geim and K. S. Novoselov, *Nature Materials*, 2007, **6**.
4. A. Eichler, J. Moser, J. Chaste, M. Zdrojek, I. Wilson-Rae and A. Bachtol, *Nature nanotechnology*, 2011, **6**, 339–342.
5. M. E. Fuentes-Perez, M. S. Dillingham and F. Moreno-Herrero, *Methods*, 2013, **60**, 113-121.
6. C. F. Quate, *Surface Science*, 1994, **299-300**, 980-995.
7. R. Garcia and A. San Paulo, *Physical Review B*, 2000, **61**, R13381-R13384.
8. A. Cerreta, D. Vobornik and G. Dietler, *European Polymer Journal*, 2013, **49**, 1916-1922.
9. A. Pyne, R. Thompson, C. Leung, D. Roy and B. W. Hoogenboom, *Small*, 2014, **10**, 3257–3261.
10. N. H. Thomson, *Ultramicroscopy*, 2005, **105**, 103-110.
11. Y. H. Yang and W. Z. Li, *Applied Physics Letters*, 2011, **98**, 041901-041903.
12. C. Leung, A. Bestembayeva, R. Thorogate, J. Stinson, A. Pyne, C. Marcovich, J. Yang, U. Drechsler, M. Despont, T. Jankowski, M. Tschöpe and B. W. Hoogenboom, *Nano letters*, 2012, **12**, 3846-3850.
13. C. Bustamante and D. Keller, *Physics today*, 1995, **48**, 33-38.
14. D. Martinez-Martin, E. T. Herruzo, C. Dietz, J. Gomez-Herrero and R. Garcia, *Physical review letters*, 2011, **106**, 198101.
15. A. Voss, C. Dietz, A. Stocker and R. W. Stark, *Nano research*, 2015.
16. S. Santos, V. Barcons, H. K. Christenson, J. Font and N. H. Thomson, *PLoS ONE*, 2011, **6**, e23821.
17. A. San Paulo and R. Garcia, *Biophysical Journal*, 2000, **78**, 1599–1605.
18. D. J. Müller and A. Engel, *Biophysical Journal*, 1997, **73**, 1633–1644.
19. A. Cerreta, D. Vobornik, G. Di Santo, S. Tobenas, L. Alonso-Sarduy, J. Adamcik and G. Dietler, *Journal of Molecular Recognition*, 2012, **25**, 486-493.

20. C.-W. Yang, I.-S. Hwang, Y. Fu Chen, C. Seng Chang and D. Ping Tsai, *Nanotechnology*, 2007, **18**, 084009.
21. F. Moreno-Herrero, J. Colchero and A. Baro, *Ultramicroscopy* 2003, **96**, 167-174.
22. A. Verdaguer, S. Santos, G. Sauthier, J. J. Segura, M. Chiesa and J. Fraxedas, *Physical Chemistry Chemical Physics*, 2012, **14**, 16080-16087.
23. H. Wang, A. B. Djurisica, W. K. Chan and M. H. Xie, *Applied Surface Science*, 2005, **252**, 1092–1100.
24. E. Palacios-Lidón, C. Munuera, C. Ocalb and J. Colchero, *Ultramicroscopy*, 2010, **110**, 789–800.
25. I. Greving, M. Cai, F. Vollrath and H. C. Schniepp, *Biomacromolecules*, 2012, **13**, 676-682.
26. M. Jaafar, A. A. A. Aljabali, I. Berlanga, R. Mas-Ballesté, P. Saxena, S. Warren, G. P. Lomonossoff, D. J. Evans and P. J. de Pablo, *ACS Applied Materials & Interfaces*, 2014, **6**, 20936-20942.
27. J. A. Irwin, H. E. Wong and I. Kwon, *Biomacromolecules*, 2013, **14**, 264-274.
28. E. T. Herruzo, A. P. Perrino and R. Garcia*Nature Communications*, 2014, **5**, 10.1038/ncomms4126.
29. J. R. Lozano and R. Garcia, *Physical Review Letters*, 2008, **100**, 076102-076105.
30. A. SanPaulo and R. Garcia, *Physical Review B*, 2001, **64**, 193411-193414.
31. F. J. Giessibl, *Physical Review B*, 1997, **56**, 16010–16015.
32. J. Israelachvili, *Intermolecular & Surface Forces*, Academic Press, 2 edn., 1991.
33. J. Tamayo and R. Garcia, *Applied Physics Letters*, 1998, **73**, 2926-2928.
34. J. P. Cleveland, B. Anczykowski, A. E. Schmid and V. B. Elings, *Applied Physics Letters*, 1998, **72**, 2613-2615.
35. M. Gauthier, R. Pérez, T. Arai, M. Tomitori and M. Tsukada, *Physical Review Letters*, 2002, **89**, 146104.
36. A. S. Paulo and R. Garcia, *Physical Review B*, 2001, **64**, 193411-193414.
37. J. Tamayo, *Appl. Phys. Lett.*, 1999, **75**, 3569-3571.
38. S. Santos, V. Barcons, J. Font and N. H. Thomson, *Nanotechnology*, 2010, **21**, 225710.
39. A. Round and M. Miles, *Nanotechnology*, 2004, **15**, S176-183.
40. H. C. Hamaker, *Physica* 1937, **4**, 1058-1072.
41. A. Raman, S. Trigueros, A. Cartagena, A. P. Z. Stevenson, M. Susilo, E. Nauman and S. A. Contera, *Nature Nanotechnology*, 2011, **6**, 809–814.
42. R. Garcia and A. San Paulo, *Physical Review B*, 1999, **60**, 4961-4967.
43. R. Garcia and A. San Paulo, *Physical Review B*, 1999, **60**, 4961.
44. S. Santos, M. Stefancich, H. Hernandez, M. Chiesa and N. H. Thomson, *The Journal of Physical Chemistry C*, 2012, **116**, 2807-2818.
45. A. Cerreta, PhD, ÉCOLE POLYTECHNIQUE FÉDÉRALE DE LAUSANNE, 2013.
46. F. J. Giessibl, F. Pielmeier, T. Eguchi, T. An and Y. Hasegawa, *Physical Review B*, 2011, **84**, 125409.
47. A. J. Katan and T. H. Oosterkamp, *The Journal of Physical Chemistry C*, 2008, **112**, 9769-9776.
48. A. Calò, N. Domingo, S. Santos and A. Verdaguer, *The Journal of Physical Chemistry C*, 2015, **119**, 8258-8265.
49. D. Dietzel, T. Mönninghoff, C. Herding, M. Feldmann, H. Fuchs, B. Stegemann, C. Ritter, U. D. Schwarz and A. Schirmeisen, *Physical Review B*, 2010, **82**, 035401.
50. G. Pletikapić, V. Žutić, I. Vinković Vrček and V. Svetličić, *Journal of Molecular Recognition*, 2012, **25**, 309-317.
51. A. N. Round, N. M. Rigby, A. Garcia de la Torre, A. Macierzanka, E. N. C. Mills and A. R. Mackie, *Biomacromolecules*, 2012, **13**, 3253-3261.
52. S. Santos, A. Verdaguer, T. Souier, N. H. Thomson and M. Chiesa, *Nanotechnology*, 2011, **22**, 465705.

53. E. Wutscher and F. J. Giessibl, *Review of Scientific Instruments*, 2011, **82**, 093703.